Conformational Features of an Actuator Containing Calix[4]arene and Thiophene: A Molecular Dynamics Study

David Zanuy,*,† Jordi Casanovas,‡ and Carlos Alemán*,†

Departament d'Enginyeria Química, E. T. S. d'Enginyeria Industrial de Barcelona, Universitat Politècnica de Catalunya, Diagonal 647, Barcelona E-08028, Spain, and Departament de Química, Escola Politècnica Superior, Universitat de Lleida, c/Jaume II N° 69, Lleida E-25001, Spain

Received: February 1, 2006; In Final Form: March 31, 2006

Molecular dynamics simulations have been performed for poly(calix[4]arene bis(bithiophene)) in dichloromethane solution. This material responds to its electronic structure variations with significant conformational changes, producing contraction−expansion movements. Simulations have been performed for the three states of this molecular actuator (reduced, oxidized−nondeprotonated, and oxidized−deprotonated), a specific force-field being developed for each case. Results, which are fully consistent with previous ab initio quantum mechanical calculations on an isolated actuating unit, have revealed important findings about the dynamics of the system. Analyses of the flexibility/rigidity of the molecular chain with the state, the interaction of the polymer with the solvent molecules and the influence of environmental factors (as the viscosity of solvent, the counterions and the thermal agitation) on the dynamics have provided important insights to the actuation mechanism.

Introduction

Within the nanotechnology context, the efficient development of molecular actuators unfolds as a fundamental goal. These active chemical systems are characterized by responding to external stimuli throughout structural distortions that can be converted into mechanical work. Normally the activating signals are electrochemical potentials, electric fields or electromagnetic waves.[1] Among all potential organic actuators, those based upon conducting organic polymers have attracted special interest of researchers.[2] The operating mechanism of such actuators is based on ions exchange in and out of the polymer matrix upon oxidation/reduction events, which induces changes in the bulk volume. The magnitude of the structural change can be regulated by the external electrochemical potential. Nonetheless, the main drawback of using conducting polymers as molecular devices comes from the low conformational flexibility of these materials, which reduces the actuator mechanism into a simple ion flux process through the supporting matrices.

Recently, a new promising type of actuator with higher conformational flexibility has been developed by combining the electrochemical capabilities of conducting polymers, specifically quarterthiophene oligomers (bis(bithiophene) units), and the conformational features of calix[4]arene scaffolds (25,27-dihydroxy-26,28-dimethoxycalix[4]arene).[3] Scheme 1 represents the basic repetitive unit of this polymeric actuator, poly(calix-[4]arene bis(bithiophene)). The effect of mixing the complex conformational flexibility of the calix[4]arene scaffolds with the electronic properties of the thiophene oligomers induces a new actuation response: instead of inducing ions diffusion, this polymeric material responds to its electronic structure variations with conformational changes, producing contraction−expansion movements.[4] This feature, conformational changes accompanying variations of the electronic state, has pointed them as potential candidates for building artificial muscles.[3,4]

SCHEME 1: Repeating unit of Poly(calix[4]arene bis(bithiophene))

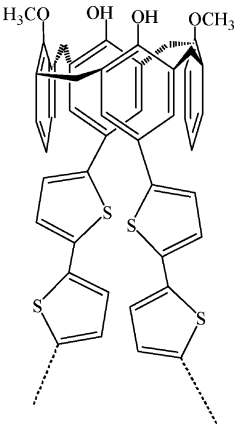

The potential impact of these materials enhanced the interest for explaining the molecular mechanism that induces the molecular expansion-contraction processes.[5,6] Scherlis and Marzari investigated in detail the role of $\pi-\pi$ interactions in the conformational movements.[5] On the other hand, in a very recent study, we were able to obtain a systematic explanation for the conformational variations that take place upon the electronic structure changes.[6] This was achieved by separating the oxidation of poly(calix[4]arene bis(bithiophene)) in two different steps: oxidation of the quarterthiophene segments and deprotonation of the two hydroxyl groups of 25,27-dihydroxy-26,28-dimethoxy calix[4]arene. In this way we located the two key interactions responsible of the actuation mechanism (Scheme 2). First, there is an expansion of the material upon oxidation due to the electrostatic repulsion of the positively charged

* Corresponding authors. E-mail: (D.Z.) david.zanuy@upc.edu; (C.A.) carlos.aleman@upc.edu.

† Departament d'Enginyeria Química, E. T. S. d'Enginyeria Industrial de Barcelona, Universitat Politècnica de Catalunya.

‡ Departament de Química, Escola Politècnica Superior, Universitat de Lleida.

10.1021/jp060680d CCC: $33.50
Published on Web 05/03/2006

SCHEME 2: Actuation mechanism of Poly(calix[4]arene bis(bithiophene))

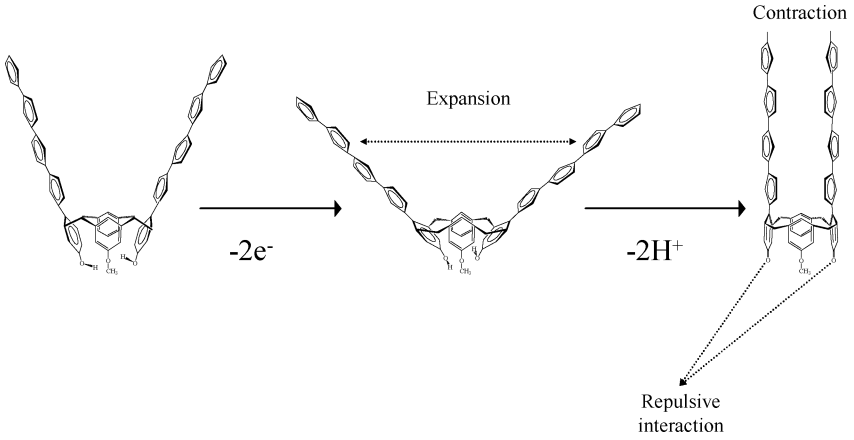

quarterthiophene blocks. After this, the dramatic contraction of the material after formation of the quinoid form by deprotonation is a consequence of the strong electrostatic repulsion between the deprotonated oxygens of the calix[4]arene units. Accordingly, the calix[4]arene scaffolds should be considered as the most active elements in the molecular actuation mechanism due to their conformational flexibility, even although the electrochemical oxidation of the thiophene oligomers is essential to promote the deprotonation of the hydroxyl groups and to control the conductivity of the polymer.

In this work we extend our previous study about the actuation mechanism of poly(calix[4]arene bis(bithiophene)), which was mainly based on the results provided by quantum mechanical calculations on an isolated actuating unit in the gas phase.[6] For this purpose, the conformational features of a molecular system constituted by several actuating units have been explored in solution, which is the experimental environment where the actuator responses take place, using molecular dynamics (MD) simulations. Force-field parameters have been explicitly developed for each electronic state involved in the mechanism (Scheme 2). A detailed analysis of the conformational dynamics has provided interesting information that improves our understanding of actuation mechanism.

Methods

All trajectories were generated using the scalable MD program NAMD 2.0.[7] Force-field parameters for the calix[4]-arene scaffold, with exception of the electrostatic ones, were obtained from an specially adapted version of AMBER99,[8] The conformation of the quarterthiophene blocks was fixed at all-anti, the van der Waals parameters being taken from the standard AMBER99 libraries.[9] The electrostatic interactions were evaluated using new sets of charges that were derived considering previously studied molecular models,[6] a specific new set of parameters being developed for each electronic state involved in the actuator response mechanism. These correspond to the reduced state (Red), the oxidized−nondeprotonated state (Ox−Ndep) and the oxidized−deprotonated state (Ox−Dep). Each set of charges was obtained by fitting the rigorously defined quantum mechanical molecular electrostatic potential, which was calculated at the HF/6-31G(d) level on a model molecule containing one complete actuating unit,[6] to the Coulombic electrostatic potential. The charges were adjusted to a chemical repetitive unit, i.e. four thiophene rings and one calix[4]arene scaffold. Quantum mechanical calculations were performed with Gaussian 03 software package.[10] Force-field parameters for the PF_6^- counterion molecules[11] were also consistent with AMBER99. Finally, the solvent structure was described using the OPLS3 model of dichloromethane.[12]

Three different poly(calix[4]arene bis(bithiophene)) systems were built, depending on the state that was about to be simulated. The molecular model considered in each case consisted of six calix[4]arene scaffolds and five quaterthiophene segments, i.e., four complete repetitive units plus two end groups each formed by a bithiophene and a calix[4]arene. Each system was placed in the center of an orthorhombic simulation box filled with 14509 dichloromethane solvent molecules, which was previously equilibrated in *NPT* conditions (temperature 298K and 1 atm of pressure). Once inside the box, those solvent molecules that overlapped any atom of poly(calix[4]arene bis(bithiophene)) were removed. For the particular case that the oligothiophene segments were positively charged, the electric neutrality of the system was reached by adding PF_6^- counterions. It should be noted that the PF_6^- molecular anion was chosen because it was experimentally characterized as acting part of the actuator before deprotonation.[3,4] After this, each system was relaxed to the experimental density value by performing new *NPT*−MD rounds with the solute frozen (Belly conditions). Each simulation box as a whole system, i.e. solute plus solvent molecules, was equilibrated a posteriori (see below). In summary, seven different trajectories were generated: two for the Red, Ox−Ndep, and Ox−Dep states, starting all six with the actuator in a conformation similar to that showed for the Red state in Scheme 2, and an extra trajectory for Ox−Dep state starting from a fully contracted conformation (see results for details).

In all simulations the bond lengths and angles of the thiophene units were kept fixed to the values obtained in quantum mechanical calculations,[6] while calix[4]arene units had only constrained their bond lengths by using the *SHAKE* algorithm.[13] Periodic boundary conditions were applied using the nearest image convention and the non bonded pair list was updated every 25 MD steps. Atom pair distance spherical-cutoffs were applied for van der Waals interactions at 14 Å; i.e. if two residues or a residue and a solvent molecule have any atom within 14 Å the interaction between the entire pair is evaluated. To avoid discontinuities in the Lennard-Jones potential a switch function was applied to allow continuum decay of energy when atom pair distances are $\geq$12 Å. For electrostatic interactions, we computed the nontruncated electrostatic potential throughout Ewald summations. The real space term was determined by the van der Waals cut off (14 Å), while the reciprocal term was estimated by interpolation of the effective charge into a charges mesh with a grid thickness of 5 points per volume unit, i.e., particle-mesh Ewald (PME) method.[14]

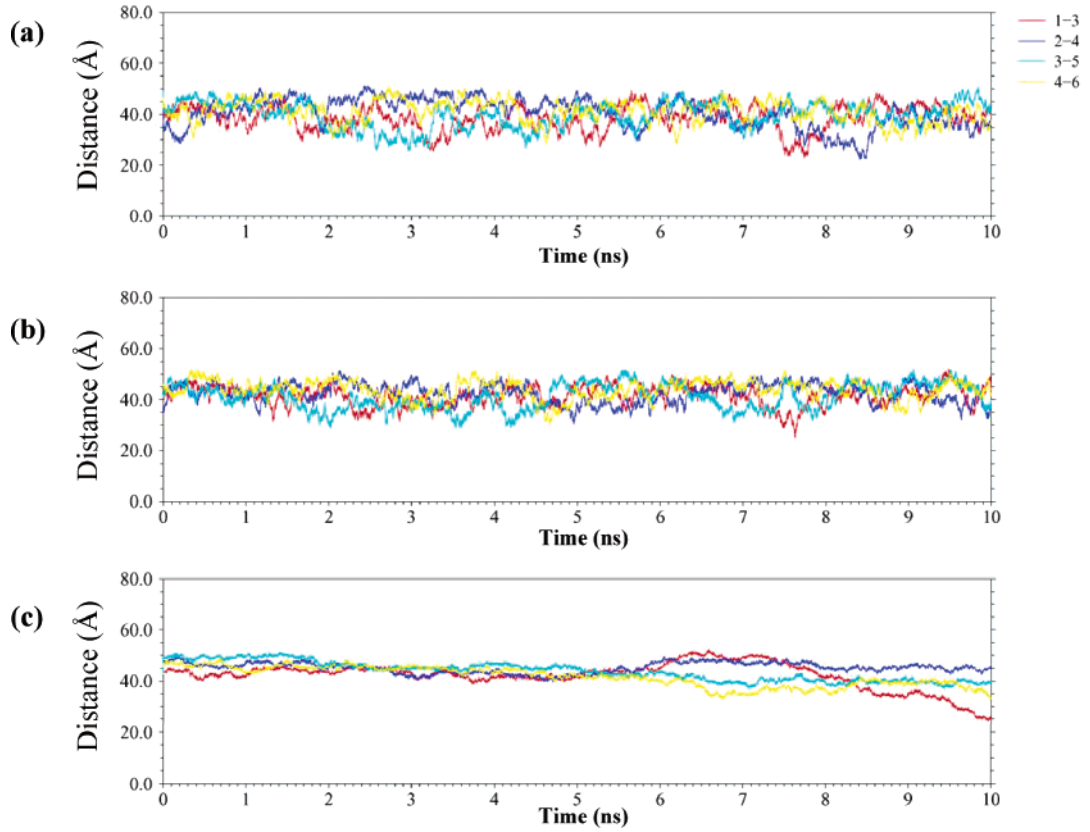

Figure 1. Time dependent evolution of the shortest distances between equivalent calix[4]arene units that are not linked to the same quaterthiophene unit. From the top to the bottom the trajectories correspond to (a) the reduced state (Red), (b) the oxidized−nondeprotonated state (Ox−Ndep), and (c) the oxidized−deprotonated (Ox−Dep).

Before any molecular dynamics trajectory was run, 1×10^4 steps of energy minimization were performed in order to relax conformational and structural tensions. In all cases, the numerical integration step was 2 fs. Different consecutive rounds of short MD runs were performed in order to equilibrate the density, temperature and pressure: 0.1 or 0.5 ns of *NVT*−MD (thermal relaxation) followed by 1 ns of isobaric relaxation (*NPT*−MD). It should be noted that in order to minimize statistical errors, two independent trajectories were run for each state, which differ in the length of the thermal relaxation (0.1 or 0.5 ns). Both temperature and pressure were controlled by the weak coupling method, the Berendsen thermobarostat,[15] using a time constant for heat bath coupling and a pressure relaxation time of 1 ps in both cases. All the *NPT*−MD production simulations were 10 ns long. Furthermore, one selected trajectory (see next section) was enlarged to 50 ns. In all cases coordinates were saved every 1000 steps (2 ps intervals) for subsequent analysis.

Results and Discussion

To describe the dynamics of the molecular actuator under study, simulations of the three states involved in the mechanism were performed using conditions mimetic to those on which experimental data were collected. Thus, classical MD experiments were performed considering explicit solvent molecules (dichloromethane), at room temperature (298 K) and 1 atm of pressure. Since calculations based on molecular mechanics do not allow electronic relaxation, three different and explicit parametrizations were developed in order to account for the main characteristics of the Red, Red−Ndep, and Red−Dep states (see Methods for details). Two different and independent trajectories were generated for each state. As the results were fully consistent in all cases, only one run will be discussed for each state. All the trajectories, independently of the state, started from an accordion-like arrangement, which was built using the results produced by quantum mechanical calculations on one actuating unit in the Red state.[6]

TABLE 1: Average[a] and Standard Deviation for Shortest Distances between Equivalent Calix[4]arene Units That Are Not Linked to the Same Quaterthiophene Units Calculated for the Different States

distances[b] (Å)	red	Ox−Ndep	Ox−Dep (accordion-like)	Ox−Dep (fully contracted)
d_{1-3}	38.6 ± 4.9	41.5 ± 4.0	42.2 ± 3.2	8.8 ± 0.6
d_{2-4}	40.6 ± 5.8	42.6 ±3.7	45.2 ± 2.1	8.7 ± 0.6
d_{3-5}	39.7 ± 5.1	41.1 ± 4.0	43.8 ± 2.7	8.8 ± 0.5
d_{4-6}	41.2 ± 4.6	43.9 ± 3.6	41.6 ± 3.8	9.0 ± 0.6

[a] All averages are after 10 ns of simulation at 298 K and 1 atm of pressure. [b] See Figure 1.

Figure 1 represents the temporal evolution of the shortest distance between pairs of calix[4]arene rings that are not directly linked to the same quarterthiophene segment (computed as centroid−centroid distance) throughout the 10 ns simulated for the three states. As can be seen in a first look, both the Red and Ox−Ndep trajectories show similar behavior, which implies that the actuator remains mainly in a extended accordion-like shape (Figure 1, a and b). Nonetheless, detailed examination reveals that the Red state tends to facilitate some breathing of the molecular chain, which is mainly due to the conformational flexibility of the calix[4]arene units that behave as the mobile hinges of the actuator. On the other hand, the conformational mobility of the Ox−Ndep state is clearly more restricted, as it was expected from the high positive charge concentration in the thiophene units. This induces high electrostatic repulsion

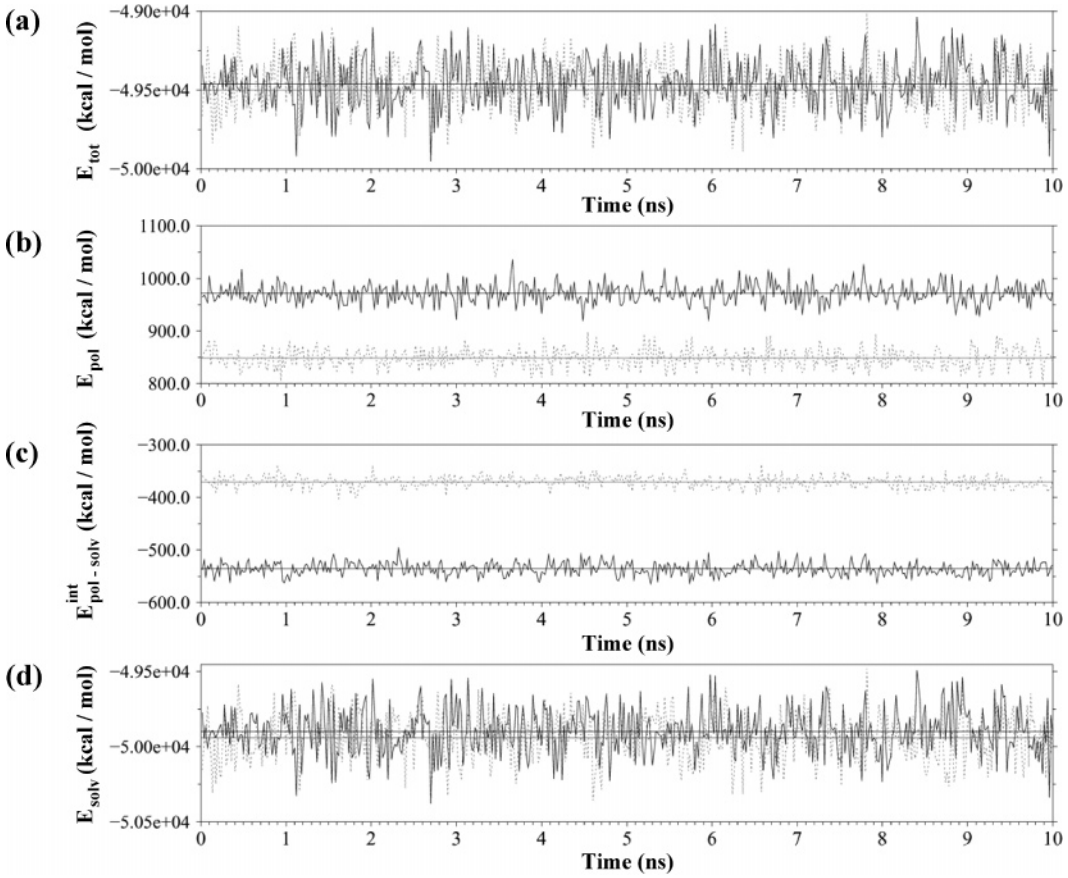

Figure 2. Energy components for the two MD performed with the Ox−Dep state: starting from the accordion-like conformation (solid line) and from the fully contracted conformation (dashed line). Time solved evolution: (a) the total energy of the system (E_{tot}); (b) the internal energy of the molecular actuator (E_{pol}); (c) the interaction energy of the polymer with the organic solvent ($E_{pol-sol}$); and (d) the cohesion energy of the solvent (E_{sol}). In each case, straight lines indicate the energy values averaged through the whole trajectories.

that prevents any meaningful approach that could occur as a consequence of the calix[4]arene dynamics. These features are consistent with the results displayed in Table 1, which lists the distances between pairs of calix[4]arene rings that are not linked to the same quartertiophene unit averaged through the whole trajectories and the corresponding standard deviations. As can be seen, the standard deviations are smaller for the Ox−Ndep state than for the Red one by 20−25%.

It is noticeable though that the conformational differences predicted in gas phase using quantum mechanics calculations on a single actuation unit[6] are bigger than the differences observed in solution for a system formed by several linked units and the corresponding counterions. The conformational differences between Red and Ox−Ndep in the present simulations are mainly manifested in terms of higher rigidity rather than the absolute value of the polymer expansion. In other words, the Ox−Ndep state would prevent the breathing of the polymeric actuator more than induce an expansion as we previously observed using other computational approaches on simple model systems.[6] Thus, the expansion predicted by the present MD simulations is of only about 5%, as is reflected in Table 1, while an expansion higher than 30% was found in our previous quantum mechanical study.[6] It is worth noting that these new specifics are consequence of a more realistic description of the molecular system and the environment. Thus, MD simulations take into account effects such as the interactions between the counterions and the polymer chain, the solvent induced screening of the electrostatic repulsions between the positively charged quarterthiophenes, the steric hindrance imposed by the viscosity of solvent and the thermal agitation. Furthermore, consideration

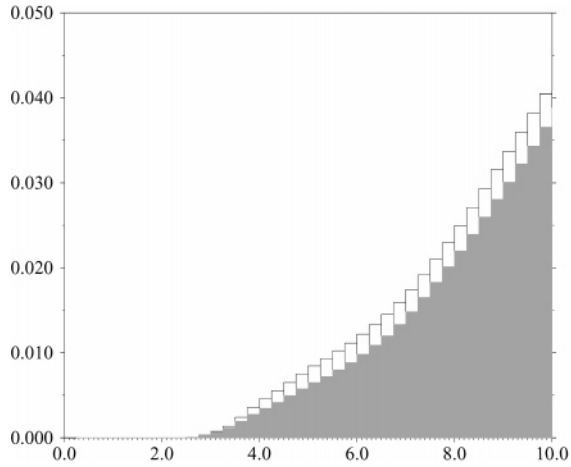

Figure 3. Radial dichloromethane distribution function (see eq 2) for the two arrangements of the polymeric actuator in the Ox−Dep state: accordion-like conformation (empty) and from the fully contracted conformation (filled).

of several linked actuation units in the polymer chain restricts the conformational flexibility of the calix[4]arene scaffolds. Additionally, for the Ox−Ndep state the conformational movements that enhance the repulsive interactions between the charged oligothiophenes are precluded. Unfortunately, the huge computational resources required by quantum mechanical calculations only allow consider small model systems.

Regarding to the Ox−Dep state, results reached after 10 ns of MD were initially unexpected. After the spectacular spontaneous contraction of the model actuating unit observed when

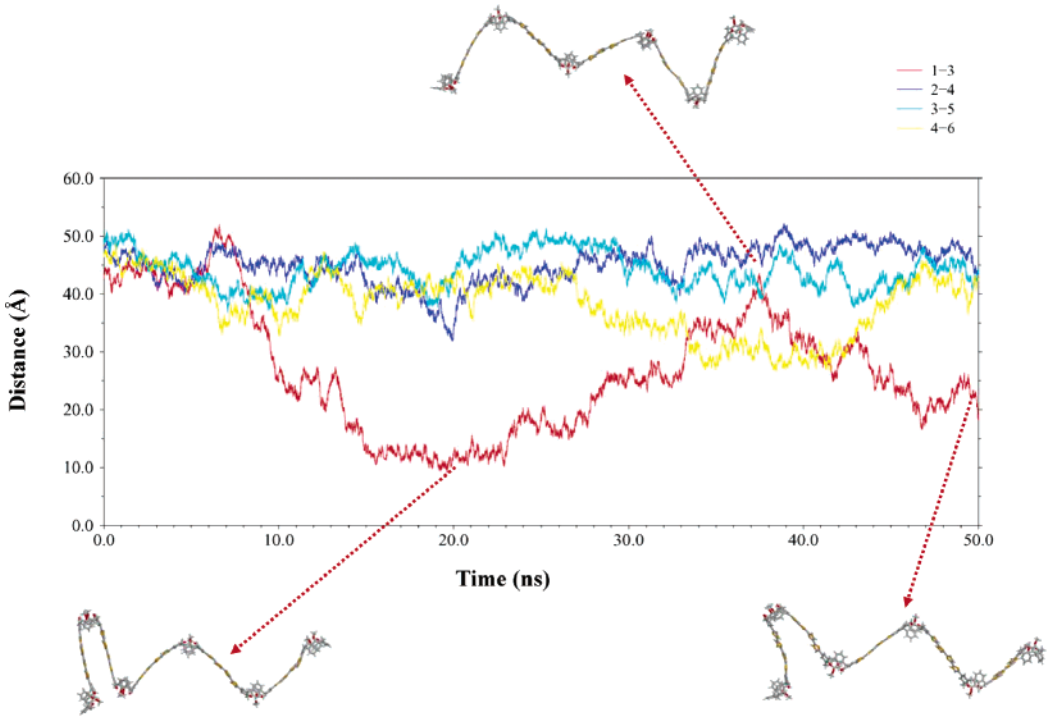

Figure 4. Time dependent evolution of the shortest distances between equivalent calix[4]arene units that are not linked to same quaterthiophene unit. The trajectory, which was started using the accordion-like arrangement, corresponds to the oxidized−deprotonated state (Ox−Dep). The structure of the polymeric actuator is displayed at selected snapshots.

optimizing its structure using first principle calculations, clear differential conformational features were expected to be seen. However, as is reflected in Figure 1c, the only significant feature is the very low amplitude of the conformational oscillations associated with the calix[4]arene scaffolds, none remarkable contraction being detected after 10 ns. Moreover, apparently this state seems even more rigid than the Ox−Ndep one. Only at the end of the simulated time frame, one of the edges of the polymeric actuator seems to start the contraction, i.e., the distance d_{1-3} slowly decreases after 7 ns of MD simulation (Figure 1c).

To get a better description of the conformational features related with the Ox−Dep state, which is responsible for the actuator contraction,[4] a new MD simulation was performed starting from a fully contracted conformation, i.e., an arrangement like that displayed in Scheme 2 for the oxidized and deprotonated actuating unit. The first remarkable feature was the total absence of conformational flexibility when the starting point was the fully contracted arrangement (Table 1). Again, the lack of conformational fluctuations seemed to show that the structural properties of the Ox−Dep state in solution might not correlate with the observations derived from quantum mechanical calculations on an isolated actuating unit. Thus, new analyses were required in order to understand our observations. From short *NPT*−MD runs it is not possible to obtain reliable thermodynamic magnitudes. However, it is relatively simple to extract significant and explicative information based on those energy terms that mainly determine the conformational dynamics.[16] Thus, the total potential energy of the system can be easily decomposed into three different terms:

$$E_{tot} = E_{pol} + E_{pol-sol} + E_{sol} \quad (1)$$

where E_{tot} is total energy of the system at any given time, E_{pol} is the internal energy of the polymer actuator, $E_{pol-sol}$ is the interaction energy between the polymer and the solvent molecules, and E_{sol} is the cohesion energy of the solvent. The relative stability of the two extreme organizations for the Ox−Dep state, the accordion-like and the fully contracted ones, can be ascertained by comparing these energy contributions.

The total energies for the trajectories started from the accordion-like and fully contracted arrangements are compared in Figure 2a, the values averaged through the whole trajectories being indicated by straight lines. The fully contracted arrangement is favored by several tenths of kcal/mol, which is what one could expect to find considering both the experimental data[5] and the recently reported mechanism.[5,6] As can be clearly noticed in Figure 2b, the fully contracted conformation is constantly more favored than the accordion-like form if only the internal energy of the polymer actuator is accounted for, this fact being fully consistent with our previous quantum mechanical results in the gas-phase.[6] However, this effect gets clearly counterbalanced by the solvation of the polymer, which is much more favored for the accordion-like arrangement (and all the potential isomorphous conformations) than for the fully contracted form (Figure 2c). Accordingly, the clue point in solution seems to be the organization of the solvent (Figure 2d): when the solvation of the actuator is less favored, the interactions between molecules of the solvent are maximized. The differences found in the E_{sol} contribution for the two trajectories suggest that the organization of the solvent depends on the conformation of the polymeric actuator. Thus, the average number of solvent molecules within a distance of 10.0 Å from any atom of the polymer is 5471 and 4738 for the accordion-like and fully contracted conformations, respectively.

To get a deeper insight about the influence of the solvation in the conformation of the polymeric actuator, the radial distribution function $g_{cm}(r)$ was calculated for the accordion-like and fully contracted conformations. This function, which provides the polymer···solvent contacts, is defined by

$$g_{cm}(r) = \frac{\langle \rho_{cm}(r) \rangle}{\rho_{cm}} \quad (2)$$

where $\rho(r)$ denotes the number density of dichloromethane molecules whose center of mass distance from an atom in the polymer is r. The average is over all the atoms and time. Results, which are displayed in Figure 3 for $r \leq 10$ Å, indicate that at distances higher than ~3.5 Å the average number of solvent molecules is higher for the accordion-like arrangement. Furthermore, the differences between the two arrangements increase with r. These features explain the differences found in Figure 2 for $E_{pol-sol}$ and E_{sol}.

The overall of the results obtained for the Ox−Dep state indicate that the accordion-like → fully contracted conformational transition is a slow process. To estimate how slow is this structural rearrangement, which is crucial for the actuation mechanism, the MD simulation of the accordion-like arrangement was enlarged to 50 ns. Results, which are displayed in Figure 4, were monitored again through the shortest distance between pairs of calix[4]arene rings that are not linked to the same quarterthiophene unit. As can be seen, this long simulation was enough to contract only one actuating unit, no other significant conformational change appearing in the other actuating units. Accordingly, these results indicate that the contraction of the molecular actuator after deprotonation is a long-time scale process. Currently simulations up to tenths of nanoseconds are feasible, but the molecular rearrangement under study requires simulations of the order of microsecond long or even higher.

It should be noted that both the viscosity of the solvent and the polymer···solvent interactions are the main responsible of the time−length scale required for the contraction of the polymeric actuator. This conclusion was reached after repeating all the simulations presented along this work in the gas-phase, i.e. neglecting all the environmental factors. The results obtained for the Red and Ox−Ndep states were very similar to those described above in dichloromethane solution. However, gas-phase MD simulations of the Ox−Dep state, using as starting point an accordion-like arrangement, led to a fast transition toward the fully contrated conformation. This drastic contraction occurred after a few nanoseconds of simulation, i.e., typically less than 5 ns. Although we are aware that gas-phase MD simulations lack physical meaning, these results allow us to confirm that the solvent plays a crucial role in the dynamics of the contraction process.

Conclusions

Results, which have been interpreted in terms of flexibility/rigidity and energy contributions produced by the bulk solvent, have allowed provide important details about the actuation mechanism. Thus, the conformational flexibility of the actuator, which is manifested by some breathing of the polymer chain, is higher in the Red state than in the Ox−Ndep state. Furthermore, the present simulations include effects that are usually neglected in quantum mechanical calculations, i.e., explicit solvent molecules, thermal effects, counterions, and a large molecular model, allowing us to correct some structural tendencies that were magnified in our previous study.[6] This is specially relevant for the Ox−Ndep state, where calculations on an isolated actuating unit predicted a significant molecular expansion with the respect to the Red state. However, dynamical calculations on a more realistic system reveal that such an expansion is moderated.

Regarding to the Ox−Dep state, the overall of the results suggest that, while the potential energy of the fully contracted arrangement is much lower than the accordion-like one, in dichloromethane solution the conformational equilibrium is finally moved toward the second organization by the increase in the amount of contacts between solvent molecules rather than the solute solubility. On the other hand, after 50 ns of MD simulation in solution, we can conclude that the accordion-like → fully contracted transition is a very slow conformational process. In summary, we have simulated the dynamics of the poly(calix[4]arene bis(bithiophene)) molecular actuator in solution considering the three states experimentally detected.

Acknowledgment. This work was supported by MCYT and FEDER funds (Project MAT2003-00251). Computer resources were generously provided by the Barcelona Supercomputer Center (BSC). D.Z. expresses thanks for financial support from the Ramon y Cajal program of the MCYT.

Supporting Information Available: Figure S1, electrostatic parameters derived for the reduced state (Red), Figure S2, electrostatic parameters derived for the oxidized−non-deprotonated state (Ox−Ndep), and Figure S3, Electrostatic parameters derived for the oxidized−deprotonated state (Ox−Dep). This material is available free of charge via the Internet at http://pubs.acs.org.

References and Notes

(1) (a) Baughman, R. H.; Cui, C.; Zakhidov, A. A.; Iqbal, Z.; Barisci, J. N.; Spinks, G. M.; Wallace, G. G.; Mazzoldi, A.; De Rossi, D.; Rinzler, A. G.; Jaschinski, O.; Roth, S.; Kertesz, M. *Science* **1999**, *284*, 1340. (b) Landi, B. J.; Raffaelle, R. P.; Heben, M. J.; Alleman, J. L.; VanDerveer, W.; Gennett, T. *Nano Lett*. **2002**, *2*, 1329.

(2) (a) Jager, E. W. H.; Inganäs, O.; Lundström, I. *Science* **2000**, *288*, 2335. (b) Lu, W.; Fadeev, A. G.; Qui, B.; Smela, E.; Mattes, B. R.; Ding, J.; Spinks, G. M.; Mazurkiewicz, J.; Zhou, D.; Wallace, G. G.; MacFarlane, D. R.; Forsyth, S. A.; Forsyth, M. *Science* **2002**, *297*, 983.(c) Otero, T. F.; Cortes, M. *Adv. Mater*. **2003**, *15*, 279.

(3) Vigalok, A.; Swager, T. M. *Adv. Mater*. **2002**, *14*, 368.

(4) Yu, H.-h.; Xu, B.; Swager, T. M. *J. Am. Chem. Soc*. **2003**, *125*, 1142.

(5) Scherlis, D. A.; Marzari, N. *J. Am. Chem. Soc*. **2005**, *127*, 3207.

(6) Casanovas, J.; Zanuy, D.; Alemán, C. *Angew. Chem., Int. Ed*. **2005**, in press.

(7) Kale, L.; Skeel, R.; Bhandarkar, M.; Brunner, R.; Gursoy, A.; Krawetz, N.; Phillips, J.; Shinozaki, A.; Varadarajan, K.; Schulten, K. *J. Comput. Phys*. **1999**, *151*, 283−312.

(8) Baaden, M.; Wipff, G.; Yaftian, M. R.; Burgard, M.; Matt, D. *J. Chem. Soc., Perkin Trans. 2* **2000**, 1315. (b) Blas, J. R.; Marquez, M.; Sessler, J. L.; Luque, F. J.; Orozco, M. *J. Am. Chem. Soc*. **2002**, *124*, 12796.

(9) Cornell, W. D.; Cieplak, P.; Bayly, C. I.; Gould, I. R.; Merz, K. M., Jr.; Ferguson, D. M.; Spellmeyer, D. C.; Fox, T.; Caldwell, J. W.; Kollman, P. A. *J. Am. Chem. Soc*. **1995**, *117*, 5179.

(10) Gaussian 03, Revision C.02, Frisch, M. J.; Trucks, G. W.; Schlegel, H. B.; Scuseria, G. E.; Robb, M. A.; Cheeseman, J. R.; Montgomery, J. A., Jr.; Vreven, T.; Kudin, K. N.; Burant, J. C.; Millam, J. M.; Iyengar, S. S.; Tomasi, J.; Barone, V.; Mennucci, B.; Cossi, M.; Scalmani, G.; Rega, N.; Petersson, G. A.; Nakatsuji, H.; Hada, M.; Ehara, M.; Toyota, K.; Fukuda, R.; Hasegawa, J.; Ishida, M.; Nakajima, T.; Honda, Y.; Kitao, O.; Nakai, H.; Klene, M.; Li, X.; Knox, J. E.; Hratchian, H. P.; Cross, J. B.; Bakken, V.; Adamo, C.; Jaramillo, J.; Gomperts, R.; Stratmann, R. E.; Yazyev, O.; Austin, A. J.; Cammi, R.; Pomelli, C.; Ochterski, J. W.; Ayala, P. Y.; Morokuma, K.; Voth, G. A.; Salvador, P.; Dannenberg, J. J.; Zakrzewski, V. G.; Dapprich, S.; Daniels, A. D.; Strain, M. C.; Farkas, O.; Malick, D. K.; Rabuck, A. D.; Raghavachari, K.; Foresman, J. B.; Ortiz, J. V.; Cui, Q.; Baboul, A. G.; Clifford, S.; Cioslowski, J.; Stefanov, B. B.; Liu, G.; Liashenko, A.; Piskorz, P.; Komaromi, I.; Martin, R. L.; Fox, D. J.; Keith, T.; Al-Laham, M. A.; Peng, C. Y.; Nanayakkara, A.; Challacombe, M.; Gill, P. M. W.; Johnson, B.; Chen, W.; Wong, M. W.; Gonzalez, C.; Pople, J. A. Gaussian, Inc.: Wallingford CT, 2004.

(11) Liu, Z.; Huang, S.; Wang, W. *J. Phys. Chem. B* **2004**, *108*, 12978.

(12) Jorgensen, W. L.; Briggs, J. M.; Contrerast, M. L. *J. Phys. Chem*. **1990**, *94*, 1683.

(13) Ryckaert, J. P.; Ciccotti, G.; Berendsen, H. J. C. *J. Comput. Phys*. **1977**, *23*, 327.

(14) Darden, T.; York, D.; Pedersen, L *J. Chem. Phys*. **1993**, *98*, 10089.

(15) Berendsen, H. J. C.; Postma, J. P. M.; van Gunsteren, W. F.; DiNola, A.; Haak, J. R. *J. Chem. Phys*. **1984**, *81*, 3684−3690.

(16) Zanuy, D.; Alemán, C. *Biomacromolecules* **2001**, *2*, 651.